5.4 APPLICATION OF THE EQUIVALENT GEOPOTENTIAL TO THE PENN STATE/NCAR MESOSCALE MODEL (MM5) FOR IMPROVING PRECIPITATION PREDICTION OVER MOUNTAINOUS REGIONS

Qiu-shi Chen, Lesheng Bai and David H. Bromwich
Polar Meteorology Group, Byrd Polar Research Center, The Ohio State University, Columbus

1[1].Introduction

Mountains have important influences on large- and mesoscale meteorology, and one of profound effects is on precipitation. An understanding of how topography modulates precipitation under a variety of large- and meso-scale conditions must be developed. Recently, Colle et al. (1999) verified the 36- and 12-km resolution Penn State/NCAR Mesoscale Model (MM5) (Grell, et al., 1993) precipitation forecasts from 9 December 1996 through 30 April 1997 and NCEP's 10-km resolution Eta Model (Eta-10) forecasts from 7 January 1997 through 30 April 1997 across the Pacific Northwest. It is found that the 12-km MM5 tends to generate too much precipitation along the steep windward slopes and not enough precipitation in the lee of major barriers. The Eta-10 overpredicts precipitation along the windward slopes even more than the 12-km MM5.

As has been understood for decades, the horizontal pressure gradient force (HPGF) in terrain-following (including pressure-based and height-based) coordinates is a small difference between two large terms over steep slopes and its computational errors are very large. This problem also arises in the nonhydrostatic model MM5 formulated in terms of perturbations relative to a reference basic state. Dempsay and Davis (1998) gave an error analysis of the MM5's HPGF schemes, and found that the standard HPGF scheme in MM5 can produce significant velocity errors above steep terrain. Some alternative schemes may reduce, but cannot eliminate, these errors. Mesinger (1984) developed the step-mountain approach of the Eta-coordinate system to calculate the pressure gradient in a region of complex terrain. However, the piecewise constant representation of the terrain is only first-order accurate in mathematics, whereas the continuous representation of the terrain in the terrain-following coordinates is at least second order accurate (depending on the chosen method of discretization). Furthermore, physical parameterizations in the planetary boundary layer are straightforward with the terrain-following coordinates.

Recently Chen and Bromwich (1999, hereafter referred to as CB99) proposed a new method to compute the HPGF in σ-coordinates and this method uses terrain-following coordinates but can eliminate large errors in computing the HPGF over steep slopes in mountainous regions. Because the horizontal wind can be separated into its irrotational and rotational parts in a limited region (Chen and Kuo, 1992a,b), the HPGF **G** in σ-coordinates is also a horizontal vector and can also be separated into its irrotational and rotational components in a limited region and expressed by

$$\mathbf{G} = -\nabla\Phi_e - \mathbf{k}\times\nabla\eta \qquad (1)$$

where Φ_e and η are referred to as equivalent geopotential and geo-streamfunction, respectively.

Recently, the MM5 (Version 2) has been used to simulate a complete annual cycle from April 1997 through March 1998 over the Greenland ice sheet by Cassano et al. (2001). The simulations are conducted by a series of 48 h duration forecasts every 24 hours, and only the forecasts of the second 24 h period are used in the statistics. The modeled precipitation distribution agrees with available accumulation observations (Csatho et al. 1997) in the interior of the ice sheet, but is excessive along the steep coastal margins of the island. The precipitation amounts predicted by the MM5 are substantially large with a maximum value in excess of 400 cm/yr compared to Csatho et al. (1997)'s analysis with a value about 120 cm/yr located on the southeast coast of Greenland. The equivalent geopotential Φ_e has been used in a generalized ω-equation in σ-coordinates, and the precipitation computed from the dynamical method (Chen et al. 1997a; Bromwich et al., 1998; CB99) for the same time period has a very good result with a maximum value in excess of 140 cm/yr on the southeast coast of Greenland. The excessive precipitation predicted by the MM5 along the steep margins of the Greenland ice sheet is similar to the problem documented by Colle et al. (1999) for forecasts along the steep windward slopes of the Cascade Mountains. In this paper, (1) is further used in the MM5 (version 3) to compute the HPGF instead of its original HPGF scheme.

2. The dynamic equations and HPGF of the MM5, and the inner and harmonic parts of the equivalent geopotential and geo-streamfunction and the internal and external HPGF

The pressure in the MM5 in z-coordinates is denoted by

$$p(x, y, z, t) = p_0(z) + p'(x, y, z, t)$$

where $p_0(z)$ is a stationary reference state, and p'(x, y, z, t) is perturbation from this state. The vertical coordinate σ is defined by

$$\sigma = \frac{p_0 - p_t}{p_s(x,y) - p_t} = \frac{p_0 - p_t}{p^*} \qquad (2)$$

where $p^*(x,y) = p_s(x, y) - p_t$, and $p_s(x, y)$ and p_t are the surface and top pressure of the stationary reference state, respectively. The pressure at a grid point is given by

$$p = p_{r0} + p' = p^*\sigma + p_t + p'$$

where $p_{r0}(x,y,\sigma)$ is the difference between p and p', and it is a stationary part in σ-coordinates and expressed by

$$p_{r0} = p - p' = p^*\sigma + p_t$$

The x- and y-components of the momentum equations in MM5 are denoted by

$$\frac{\partial(u/m)}{\partial t} + \frac{1}{\rho}\left(\frac{\partial p'}{\partial x} - \frac{\sigma}{p^*}\frac{\partial p^*}{\partial x}\frac{\partial p'}{\partial \sigma}\right) = F_x \qquad (3)$$

$$\frac{\partial(v/m)}{\partial t} + \frac{1}{\rho}\left(\frac{\partial p'}{\partial y} - \frac{\sigma}{p^*}\frac{\partial p^*}{\partial y}\frac{\partial p'}{\partial \sigma}\right) = F_y \qquad (4)$$

where F_x and F_y are advection and other terms. The HPGF in (3) and (4) is expressed by

[1] Corresponding author address: Qiu-Shi Chen, Byrd Polar Research Center, The Ohio State University, 1090 Carmack Rd., Columbus, OH 43210; E-mail: qchen@polarmet1.mps.ohio-state.edu

$$\mathbf{G} = -\frac{1}{\rho}\left(\nabla p' - \frac{\sigma}{p^*}\frac{\partial p'}{\partial \sigma}\nabla p^*\right) = -\frac{1}{\rho}(\nabla p' - \tau \nabla p_{r0}) \quad (1a)$$

where

$$\tau = \frac{1}{p^*}\frac{\partial p'}{\partial \sigma} = \left(\frac{\partial p_{r0}}{\partial \sigma}\right)^{-1}\frac{\partial p'}{\partial \sigma}$$

If the HPGF (1a) is separated into the rotational and irrotational parts as in (1.1), the equivalent geopotential Φ_e and the geo-streamfunction η satisfy the Poisson equations

$$\nabla^2\phi_e = \frac{\partial}{\partial x}\left(\frac{1}{\rho}\frac{\partial p'}{\partial x}\right) + \frac{\partial}{\partial y}\left(\frac{1}{\rho}\frac{\partial p'}{\partial y}\right) - \left\{\frac{\partial}{\partial x}\left(\frac{\tau}{\rho}\frac{\partial p_{r0}}{\partial x}\right) + \frac{\partial}{\partial y}\left(\frac{\tau}{\rho}\frac{\partial p_{r0}}{\partial y}\right)\right\} \quad (5)$$

$$\nabla^2\eta = \frac{\partial}{\partial x}\left(\frac{1}{\rho}\right)\frac{\partial p'}{\partial y} - \frac{\partial}{\partial y}\left(\frac{1}{\rho}\right)\frac{\partial p'}{\partial x} - \left\{\frac{\partial}{\partial x}\left(\frac{\tau}{\rho}\frac{\partial p_{r0}}{\partial y}\right) + \frac{\partial}{\partial y}\left(\frac{\tau}{\rho}\frac{\partial p_{r0}}{\partial x}\right)\right\} \quad (6)$$

Over the globe, the above Poisson equations are easily solved without lateral boundary conditions. If they are solved in a limited region, the boundary condition is expressed by

$$\mathbf{s}\bullet\mathbf{G} = \frac{\partial \eta}{\partial n} + \frac{\partial \phi_e}{\partial s} = G_t = -\frac{1}{\rho}\frac{\partial p'}{\partial s} + \frac{\tau}{\rho}\frac{\partial p_{r0}}{\partial s} \quad (7)$$

$$\mathbf{n}\bullet\mathbf{G} = -\frac{\partial \eta}{\partial s} + \frac{\partial \phi_e}{\partial n} = G_n = -\frac{1}{\rho}\frac{\partial p'}{\partial n} + \frac{\tau}{\rho}\frac{\partial p_{r0}}{\partial n} \quad (8)$$

where **s** and **n** are tangential and normal unit vectors, respectively, and s and n are distances along and normal to the boundary. In this case, the equivalent geopotential and geo-streamfunction are derived by solving Poisson equations (5) and (6) with the coupled boundary conditions (7) and (8).

Using the harmonic-sine series, the solutions for Φ_e and η can be separated into their inner and harmonic parts as

$$\Phi_e = \Phi_{ei} + \Phi_{eh}, \qquad \eta = \eta_i + \eta_h \quad (9)$$

where Φ_{eh}, η_h and Φ_{ei}, η_i are the harmonic and inner parts of the equivalent geopotential and the geo-streamfunction, respectively. The inner parts Φ_{ei} and η_i satisfy Poisson equations (5) and (6) with zero Dirichlet boundary value. The solutions of Φ_{ei} and η_i can easily be derived by using the double Fourier sine series. The internal HPGF is then computed by

$$G_{xI} = -\frac{\partial \eta_i}{\partial y} + \frac{\partial \phi_{ei}}{\partial x}, \qquad G_{yI} = \frac{\partial \eta_i}{\partial x} + \frac{\partial \phi_{ei}}{\partial y} \quad (10)$$

where G_{xI} and G_{yI} are the components of the internal HPGF.

In a limited region, the difference between the HPGF and internal HPGF is denoted by

$$G_{xE} = G_x - G_{xI} = -\frac{1}{\rho}\frac{\partial p'}{\partial x} + \frac{\tau}{\rho}\frac{\partial p_{r0}}{\partial x} - G_{xI} \quad (11)$$

$$G_{yE} = G_y - G_{yI} = -\frac{1}{\rho}\frac{\partial p'}{\partial y} + \frac{\tau}{\rho}\frac{\partial p_{r0}}{\partial y} - G_{yI} \quad (12)$$

and G_{xE} and G_{yE} are referred to as the components of the external HPGF. Utilizing (1), (9) and (10), the external HPGF can be expressed by the harmonic parts of the equivalent geopotential and the geo-streamfunction as

$$G_{xE} = -\frac{\partial \eta_h}{\partial y} + \frac{\partial \phi_h}{\partial x}, \qquad G_{yE} = \frac{\partial \eta_h}{\partial x} + \frac{\partial \phi_{hi}}{\partial y} \quad (13)$$

The harmonic parts of the equivalent geopotential and the geo-streamfunction satisfy the Laplace equations

$$\nabla^2\phi_{eh} = 0, \qquad \nabla^2\eta_h = 0 \quad (14)$$

Thus, the external HPGF is not only non-divergent but also irrotational in a limited region. The coupled boundary conditions (7) and (8) for solving Laplace equations (14) of the harmonic parts in region R become

$$\frac{\partial \eta_h}{\partial n} + \frac{\partial \phi_{eh}}{\partial s} = G_{Et} = -\frac{1}{\rho}\frac{\partial p'}{\partial s} + \frac{\tau}{\rho}\frac{\partial p_{r0}}{\partial s} - G_{It} \quad (15)$$

$$-\frac{\partial \eta_h}{\partial s} + \frac{\partial \phi_{eh}}{\partial n} = G_{En} = -\frac{1}{\rho}\frac{\partial p'}{\partial n} + \frac{\tau}{\rho}\frac{\partial p_{r0}}{\partial n} - G_{In} \quad (16)$$

where G_{Et} and G_{En} are the tangential and normal components of the external HPGF, $\mathbf{G}_E$, at the boundary.

3. The HPGF computed from a reconstruction method and comparison of the analyses and the outputs of the predicted results with and without the equivalent geopotential over mountainous regions

The topography of Greenland with steep slopes near its coast is shown in Fig. 1. As synoptic example, the sea-level pressure (SLP) map on 0000 UTC, 1 February 2001 is shown in Fig. 2. Data are obtained from NCEP at $1^0\times1^0$ resolution and interpolated to 23 σ levels where top level is at 100 hPa. The grid spacing is 40 km. The inner parts of the equivalent geopotential and geo-streamfunction are derived from Poisson equations (7) and (8) with zero Dirichlet boundary values, and these inner parts at σ=0.995 are shown in Figs. 3 and 4, respectively. Because the HPGF, $-\nabla\phi$(x,y,p,t) in p-coordinates is also irrotational, the equivalent geopotential ϕ_e (x, y, σ, t) in σ-coordinates can be used in the same way as ϕ(x, y, p, t) is used in p-coordinates. The equivalent geopotential ϕ_e can be used in synoptic analysis on constant σ surface. In Fig. 2, some artificial anomalous systems exist over Greenland in the SLP map caused by pressure reduction to the sea level, but they are not present in the analyses at σ =0.995 in Fig. 3, and weather systems over Greenland are shown smoothly on the σ-surface analyses. The geostrophic relation $\phi_e = f_0\psi$ between the equivalent geopotential and rotational wind on the constant σ surface for the synoptic scale motions is the same as that $\phi = f_0\psi$ on the isobaric surface.

In p-coordinates, the HPGF $-\nabla\Phi$ (x, y, p, t) has only the irrotational part, and its rotational part, (corresponding to $-\mathbf{k}\times\nabla\eta$), can only be computed through the lower boundary condition at the earth's surface and expressed implicitly. The rotational part is much smaller than the irrotational part shown in Figs. 3 and 4, thus the small difference between two large terms over steep slopes is eliminated automatically.

The components of the internal HPGF, G_{xI} and G_{yI}, can be computed from (10), and those of the external HPGF, G_{xE} and G_{yE}, are computed from (11) and (12). Within region R, the external HPGF, $\mathbf{G}_E$, is both irrotational and nondivergent, and it satisfies

$$-\frac{\partial G_{xE}}{\partial y} + \frac{\partial G_{YE}}{\partial x} = 0, \qquad \frac{\partial G_{xE}}{\partial x} + \frac{\partial G_{yE}}{\partial y} = 0 \quad (17)$$

Differentiating the first and second equations of (17) with respect to x and y, respectively, the following Laplace equations for G_{xE} and G_{yE}, are derived as

$$\nabla^2 G_{xE} = 0, \qquad \nabla^2 G_{yE} = 0 \qquad (18)$$

Thus, the components of the external HPGF, G_{xE} and G_{yE}, are harmonic functions themselves, and do not have maximum and minimum within region R and attain their extreme values at the boundary.

Because the external HPGF is both irrotational and nondivergent, based on Chen and Kuo (1992b), its two components at the boundary

$$G_{xE}|_{\Sigma} = G_{xE}(\Sigma), \qquad G_{yE}|_{\Sigma} = G_{yE}(\Sigma) \qquad (19)$$

must satisfy the consistency condition. As pointed out by Chen et al. (1996), the method of solving two Laplace equations (18) with the given boundary values (19) to derive the external HPGF is referred to as a direct method. This direct method can accurately be used to reconstruct the external HGGF under the condition that the prescribed boundary values (19) satisfy the consistency condition. There are several methods to reconstruct the HPGF from Φ_e and η in a limited region (Chen and Kuo 1992a), the direct method is the simplest one. If the prescribed boundary values $G_{xE}(\Sigma)$ and $G_{yE}(\Sigma)$ do not satisfy the consistency condition, the direct can also be used, but in this case the derived external HGGF may no longer be both irrotational and nondivergent and have some errors due to the inconsistency boundary condition.

The external HGGF reconstructed by the direct method under the boundary values (19) is expressed by G_{xE}' and G_{yE}', and then the HPGF is derived by

$$G_x = G_{xE}' + G_{xI} \qquad G_y = G_{yE}' + G_{yI} \qquad (20)$$

This method is used in the MM5 to compute the HPGF instead of the original method (1a). The 36h predicted SLP and output ϕ_{ei} at σ=0.995 from the MM5 are shown in Figs. 5 and 6, respectively. The 36h precipitation prediction of the MM5 without ϕ_e is shown in Fig.7, it is substantially large over the southeast of Greenland. The predicted precipitation errors are greatly reduced by using (1) without other changes. The difference between the component G_x of the HPGF computed by (1) and (1a) at σ=0.87 at 24h after the initial time is shown in Fig. 8. The G_x computed by (1) is smaller than by (1a) in the windward steep slopes.

4. Conclusion

There are several important advantages to using (1). The first is that the HPGF in σ-coordinates is computed accurately. Based on the tests of the computed HPGF over Greenland, the major differences between the original scheme of MM5 and (1) are located over the steep slopes. Tests of the simulated precipitation by using (1) in the MM5 without other changes show that the precipitation errors over the steep slopes of Greenland are improved.

The second advantage is that Φ_e can be used in synoptic analysis and model outputs directly on constant σ surfaces and in the same way as Φ(x, y, p, t) is used in p-coordinates. The modeled results are not necessary to transfer to p-coordinates and can be compared with the observed analyses directly in σ-coordinates. The artificial anomalous systems over Greenland on the sea-level pressure maps and the lower tropospheric isobaric surfaces are not present, and weather systems over high mountain regions are shown more smoothly and correctly on the σ surfaces.

Acknowledgments This research was sponsored by NASA grant NAG5-10601.

Reference

Bromwich, D. H., Q.-S. Chen, Y. Li, and R. I. Cullather, 1999: Precipitation over Greenland and its relation to the North Atlantic Oscillation. *J. Geophys. Res*., **104** (D18), 22,103 - 22,115.

Cassano, J. J., J. E. Box, D. H. Bromwich, L. Li, and K. Steffen, 2001: Verification of Polar MM5 simulations of Greenland's atmospheric circulation. *J. Geophys. Res.*, (In press).

Chen, Q.-S., and Y.-H. Kuo, 1992a: A harmonic-sine series expansion and its application to the partitioning and reconstruction problem in a limited area. *Mon. Wea. Rev*., **120**, 91-112.

Chen, Q.-S., and Y.-H. Kuo, 1992b: A consistency condition for the wind field reconstruction in a limited area and a harmonic-cosine series expansion. *Mon. Wea. Rev*., **120**, 2653-2670.

Chen, Q.-S., Y.-H. Kuo and D. H. Bromwich, 1996: A balanced ageostrophic initialization with a fixed external wind boundary value for limited-area models. *J. Meteor. Soc. Japan,* **74**, 325-342.

Chen, Q.-S., D. H. Bromwich and L. Bai, 1997: Precipitation over Greenland retrieved by a dynamic method and its relation to cyclonic activity. *J. Climate*, **10**, 839-870.

Chen, Q.-S., and D. H. Bromwich, 1999: An equivalent isobaric geopotential height and its application to synoptic analysis and to a generalized ω-equation in σ-coordinates. *Mon. Wea. Rev.,* **127**, 145-172.

Colle B. A., K. J. Westrick, and C. F. Mass, 1999: Evaluation of MM5 and Eta-10 precipitation forecasts over the Pacific Northwest during the cool season. *Weather and Forecasting,* **14**, 137-154.

Csathò, B., H. Xu, R. Thomas, D. H. Bromwich, and Q.-S. Chen, 1997: Comparison of accumulation and precipitation maps of the Greenland Ice Sheet, *EOS. Trans. AGU*, **78**(46), Fall. Meet. Suppl., F9.

Dempsey, D. and C. Davis, 1998: Error analyses and test of pressure gradient force schemes in nonhydrostatic, mesoscale model. *Preprints, 12th Conf. on Numerical Weather Prediction,* 11-16 January 1998, Phoenix, AZ, Amer. Meteor. Soc., 236-239.

Grell, G. A., J. Dudhia, D. R. Stauffer, 1993: A description of the fifth generation Penn State/NCAR mesoscale model. *NCAR Tech. Note* 398+IA, 122pp.

Mesinger, F., 1984: A blocking technique for representation of mountains in atmospheric models. *Rev. Meteorol. Aeronautica,.* **44,** 195-202.

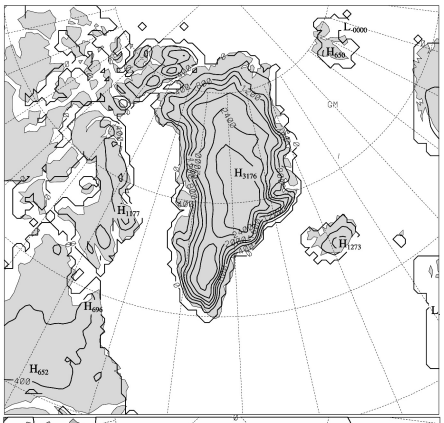

Fig. 1. The topography of Greenland and adjacent areas (in m with a contour interval of 400 m).

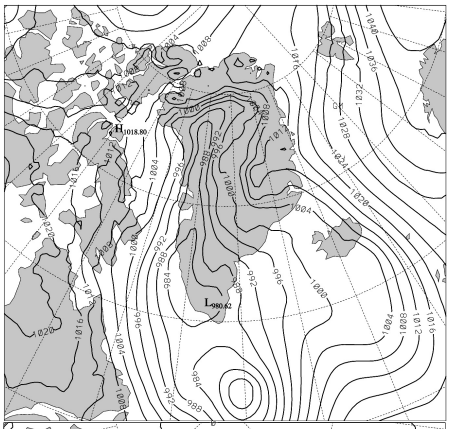

Fig. 2. The sea level pressure (at 4 hPa spacing) at 0000 UTC 1 February 2001.

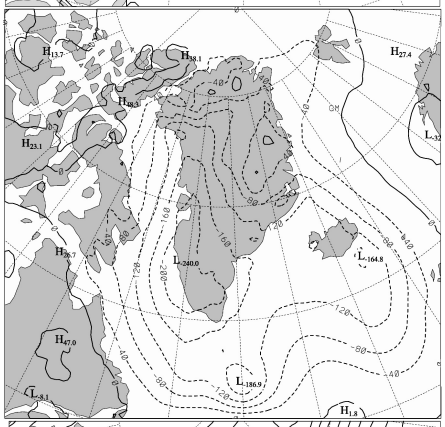

Fig. 3 The inner part of the equivalent geopotential at 0000 UTC 1 February 2001 at σ=0.995 (in 10 $m^2 s^{-2}$ and contour interval: 40x10 $m^2 s^{-2}$)

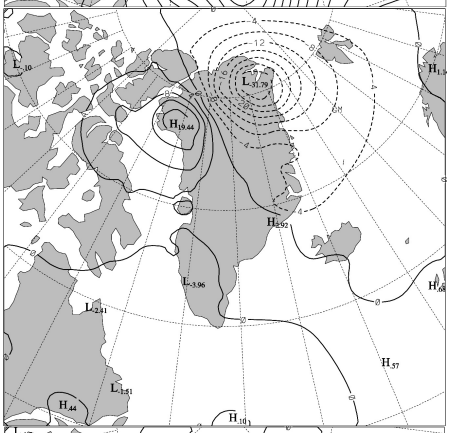

Fig. 4 Same as Fig. 3 but for the inner part of the geo-streamfunctio n. (in 10 $m^2 s^{-2}$ and contour interval: 4x10 $m^2 s^{-2}$)

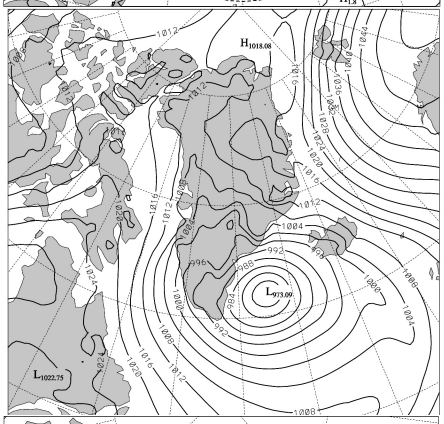

Fig. 5 The 36h predicted sea level pressure (at 4 hPa spacing) from the initial time (0000 UTC 1 February 2001) by the MM5.

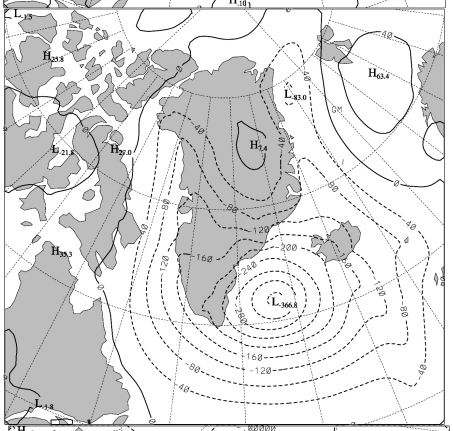

Fig. 6 The 36h predicted inner part of the equivalent geopotential from the initial time (0000 UTC 1 February 2001) by the direct output at σ=0.995 from the MM5 Same as Fig. 3 $m^2 s^{-2}$).

Fig. 7 The 36h total precipitation prediction (at 0.6 cm spacing) from the initial time (0000 UTC 1 February 2001) by the MM5 without the equivalent geopotential.

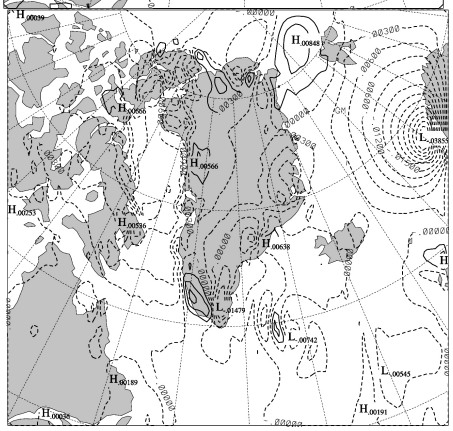

Fig. 8 The distribution of the difference between the x-component G_x of the HPGF computed by (1) and (1a) at σ=0.87 at 24h after the initial time (0000 UTC 1 February 2001).